NEW CONSTRAINTS ON THE MAJOR NEUTRON SOURCE FOR *s*-PROCESS NUCLEOSYNTHESIS IN AGB STARS. N. Liu[1,2], R. Gallino[3], A. M. Davis[4], R. Trappitsch[4,5], T. Stephan[4], P. Boehnke[4], L. R. Nittler[2], C. M. O'D. Alexander[2], and M. Pellin[4,6], [1]Department of Physics, Washington University in St. Louis, St. Louis, MO 63130, USA, nliu@physics.wustl.edu, [2]Department of Terrestrial Magnetism, Carnegie Institution for Science, Washington, DC 20015, USA, [3]Dipartimento di Fisica, Università di Torino, Torino 10125, Italy, [4]The University of Chicago, Chicago, IL 60637, USA, [5]Lawrence Livermore National Laboratory, CA 94550, USA, [6]Argonne National Laboratory, Argonne, IL 60439, USA.

Introduction: Asymptotic Giant Branch (AGB) stars are the stellar site for the main *s*-process (slow neutron capture process), with ^{13}C being the major neutron source via $^{13}C(\alpha,n)^{16}O$ [1]. Formation of ^{13}C via $^{12}C(p,\gamma)^{13}N(\beta^{+}\nu)^{13}C$ within the so-called "^{13}C-pocket" requires mixing protons from the convective H envelope into the radiative He intershell, a locally unstable thermodynamic state that is extremely difficult to treat in stellar models, because many physical mechanisms may compete in the pocket formation.

Presolar grains are ancient stellar relicts, and a majority of presolar SiC grains, the mainstream (MS) grains, came from low-mass AGB stars with *s*-process isotopic signatures. The rare Y and Z grains also originated in AGB stars, but of lower metallicity. In our previous investigation of ^{13}C-pocket uncertainties, we obtained correlated Sr and Ba isotope ratios in single SiC grains, and the data consistently point to the existence of large ^{13}C-pockets in AGB stars [2,3,4]. However, a recent study [5] showed that these ^{13}C-pocket characteristics failed to match Ni isotopic data from MS grains. The reason for this disagreement is unclear, but may be partially because the Torino AGB stellar model adopted in [5] had several improvements compared to the one used in [4]. Here, we investigate this problem by comparing the literature MS grain isotope data on Sr, Ba, and Ni to the updated Torino AGB models with the main aim of testing the recently proposed large ^{13}C-pocket produced by magnetohydrodynamic simulations in [6] (hereafter T17 pocket). We also report new Sr, Mo, and Ba isotope data for a large number of Y and Z grains to investigate the characteristics of ^{13}C-pockets in AGB stars with varying metallicities.

Experiments & Models: Detailed descriptions of Torino AGB models can be found in [2–5]. In this study, we adopted the simulated T17 pocket in our post-processing *s*-process calculations and also varied the ^{13}C concentration in the pocket to search for the best match to the presolar grain data (Fig. 1). Note that the T17 ^{13}C-pocket has a quite flat ^{13}C profile within the pocket and is, therefore, similar to the largest-sized ^{13}C-pocket (hereafter L15 pocket) discussed by [4, Fig. 9h]. To better understand the ^{13}C-pockets in lower-metallicity AGB stars, we also analyzed 42 sub-µm- to µm-sized Y and Z grains for their Sr, Mo, and Ba isotopic compositions with CHILI [8]; 15 MS grains were also measured during the same session (Fig. 2). These grains had been measured with a NanoSIMS 50L instrument at Carnegie for their C, N, and Si isotope ratios prior to the CHILI analysis. We obtained Mo isotope ratios in all 42 grains; Sr and Ba isotope ratios were obtained in only about one-third of the grains, indicating lower efficiencies of the Sr and Ba resonance ionization schemes and/or lower Sr and Ba concentrations in the grains.

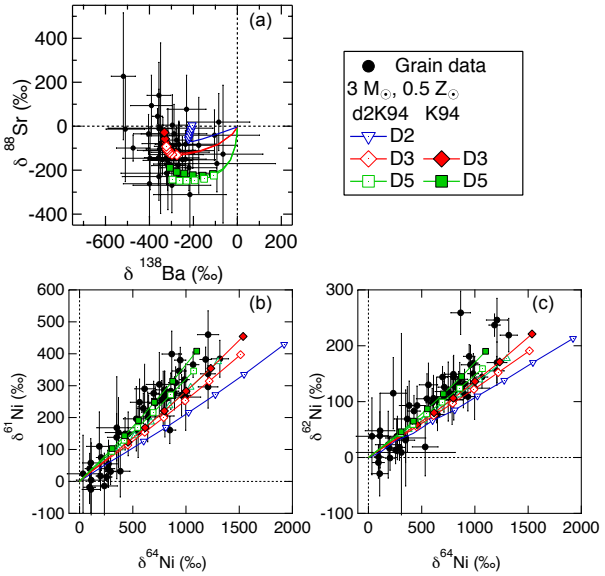

Fig. 1. Comparison of MS grain data [2–5] to Torino AGB model calculations for a 3 $M_{\odot}$, 0.5 $Z_{\odot}$ AGB star by adopting the T17 ^{13}C-pocket. Each model prediction evolves from zero (initial stellar composition) along colored lines, with symbols plotted on top of the lines when C/O>1 in the envelope. K94 refers to the $^{22}Ne(\alpha,n)^{25}Ne$ rate recommended by [7] and d2K94 represents the K94 rate reduced by a factor of two. The cases of D2, D3, D5 refer to the ^{13}C concentration (original case) in the T17 pocket divided by a factor of two, three, and five.

MS Grain Constraint: Figure 1a shows that the new AGB stellar model requires a ^{13}C-pocket larger than previously constrained for matching the grain data. Based on the old stellar model, [4] showed that with increasing pocket size, the model predictions for δ^{88}Sr continue to increase, and the best match to the grain data is reached by model predictions with a ^{13}C-pocket size four times smaller than that of the L15 pocket (hereafter L15_d4 pocket) during the C-rich phase, whilst model predictions with the L15 pocket yield the

poorest match to the data due to the rapidly growing δ^{88}Sr values with increasing thermal pulses (TPs). In contrast, the new calculations (Fig. 1a) show that the T17 pocket, similar to the L15 pocket, can explain the Sr-Ba isotope data. The significant reduction in the predictions for δ^{88}Sr mainly results from the incorporation of C-enhanced molecular opacities in the new stellar model, which induces lower stellar temperatures and enhanced mass loss rates. This results in less efficient operation of the ^{22}Ne(α,n)^{25}Mg source and consequently reduced ^{86}Sr depletion in AGB stars, because the ^{86}Sr nuclei produced in the ^{13}C-pocket are partially destroyed during the peak neutron density induced by the marginal activation of the ^{22}Ne(α,n)^{25}Mg reaction at the bottom of the He-burning zone during a TP. This effect can be observed in Fig. 1a by comparing d2K94 with K94 calculation results. Also, this explains the better match given by model predictions for a 3 $M_{\odot}$ AGB star with respect to those for a 2 $M_{\odot}$ AGB star (adopted in previous studies) because of its increased stellar temperature.

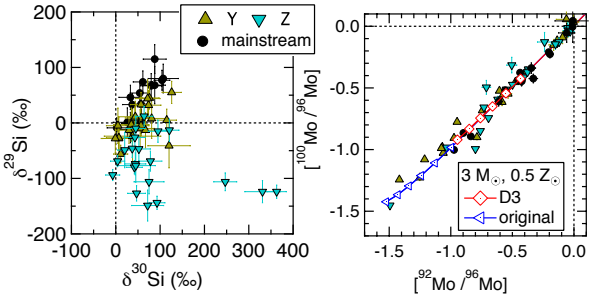

Fig. 2. Three-isotope plots of grain data from this study. The Mo isotope ratios are shown as the $\log_{10}$ of the solar system normalized isotope ratios instead of δ notations. Errors are 2σ. The original case refers to the ^{13}C concentration in the T17 pocket given in [6].

The Sr-Ba isotope data constrains the ^{13}C concentration to lie between the D5 and D2 cases in the T17 pocket, which also provide reasonable matches to the Ni isotope data in Figs. 1(b) & (c). In contrast, by adopting a smaller ^{13}C-pocket (four times smaller than the T17 pocket) in the new Torino AGB models, the D6 case best reproduces the slopes in the three Ni isotope plots (Fig. 11 in [5]), while the D2 case provides the best match to the grain concentrated region in the Sr-Ba isotope plot (not shown). Thus, we can conclude that the discrepancy between the constraints from the correlated Sr-Ba and Ni isotope data is not a result of different stellar models. Instead, the Sr-Ba and Ni data can be explained by adopting a larger ^{13}C-pocket with flattened ^{13}C concentrations, providing support for the large T17 pocket but probably with a reduced ^{13}C concentration. The grain-model agreement in Fig. 1 can be further improved if MS grains came from more massive AGB stars with higher stellar temperatures so that the ^{22}Ne(α,n)^{25}Mg reaction can operate more efficiently, producing higher δ^{88}Sr values in Fig. 1(a) as well as steeper slopes in Figs. 1(b) & (c).

Y/Z Grain Constraint: Y and Z grains have higher ^{30}Si excesses than MS grains, which likely indicates their origins from AGB stars with lower metallicities relative to the parent stars of MS grains by about a factor of 2−3 (e.g., [9]). We found *s*-process Mo isotopic compositions in 18 of 21 Y, 18 of 21 Z, and 12 of 15 MS grains (Fig. 2). Assuming that the *s*-process indeed operated efficiently in all AGB stars, the normal Mo isotopic compositions measured in some grains probably indicate that up to 20% of grains suffered from severe Mo contamination.

Figure 2 shows that the most anomalous Mo isotope ratios observed in Y and Z grains are more extreme than those of MS grains. Since the *s*-process should in principle operate more efficiently in lower-metallicity AGB stars because of enhanced neutron/seed ratios, the more anomalous Mo isotope ratios of Y and Z grains support the conclusion that their parent AGB stars had lower metallicities than the parent stars of MS grains. In addition, the difference in the *s*-process endmember between Y/Z and MS grains can be explained by the difference between the original and D3 cases, respectively (Fig. 2). Since the *s*-process efficiency is a function of the neutron/seed ratio, the model predictions in the original case for a 0.5 $Z_{\odot}$ AGB star are similar to those in the D3 case for a 0.177 $Z_{\odot}$ AGB star, except for the slightly higher stellar temperature of the latter. Thus, comparison of grain data to the new Torino AGB models with the T17 pocket implemented for Mo isotope ratios also implies that Y and Z grains came from AGB stars with metallicities up to three times lower than the metallicities of MS grain parent AGB stars, which is consistent with the constraints from light-element isotopic data.

Conclusion: We found that a large ^{13}C-pocket with flattened ^{13}C concentrations is required to consistently explain previous MS grain data on Sr, Ba, and Ni isotopes, which provides support for the dominant role of magnetic buoyancy in forming the ^{13}C-pocket; a reduced ^{13}C concentration could be achieved by additional mixing process(es), as a result of e.g., the stellar rotation motion. In addition, the T17 pocket can also be used to well explain the Mo isotope data of MS, Y, and Z grains, which likely implies the universality of ^{13}C-pockets in AGB stars with varying metallicities.

References: [1] Gallino R. et al. (1998) *ApJ, 497,* 388–403. [2] Liu N. et al. (2014a) *ApJ*, *786*, #66 (20pp). [3] Liu N. et al. (2014b) *ApJ*, *788*, #163 (7pp). [4] Liu N. et al. (2015) *ApJ*, *803*, #12 (23pp). [5] Trappitsch R. et al. (2018) *GCA*, *221*, 87−108. [6] Trippella O. et al. (2017) *ApJ*, *818*, #125 (9pp). [7] Käppeler F. et al. (1994) *ApJ*, *437*, 396−409. [8] Stephan et al. (2016) *IJMS*, *407*, 1−15. [9] Amari S. et al. (2001) *ApJ*, *546*, 248−266.

LLNL-ABS-744240.